journal

Experimental Evidence for the Development of Bimodal Grain Size Distributions by the Nucleation-Limited Coarsening Mechanism

Tomoko Sano[*,‡] and Gregory S. Rohrer[*,†]

Department of Materials Science and Engineering, Carnegie Mellon University, Pittsburgh, Pennsylvania 15213-3890

It has recently been hypothesized that transient bimodal grain size distributions can arise from unimodal distributions during coarsening if the continued growth of a majority fraction of the crystals is arrested by the energy barrier to nucleate new layers. To test this hypothesis experimentally, $SrTiO_3$ has been coarsened in a titania-rich liquid at 1500°C. Measurements of the grain size distribution as a function of time show a transient bimodal distribution that consists of a constant number of larger grains growing many times faster than a decreasing number of much smaller grains. The observations are consistent with the nucleation-limited coarsening theory, which provides a plausible explanation for the development of transient bimodal grain size distributions in systems of crystals bounded by singular surfaces.

I. Introduction

THE origin of transient bimodal grain size distributions (frequently referred to as abnormal grain growth) that appear during the coarsening of crystals in the presence of a liquid phase has been the subject of a considerable debate. The classical theories for diffusion-limited coarsening,[1,2] surface attachment-limited coarsening,[2] and ledge migration-limited coarsening[3] all produce relatively narrow, steady-state, unimodal grain size distributions. Although the classical theories assume a zero volume fraction for the coarsening phase and an isotropic surface energy, relaxing these constraints does not allow the development of a bimodal grain size distribution.[4–11] However, it has recently been hypothesized that if coarsening is limited by the nucleation of new terraces on singular surfaces, then conditions exist where a transient bimodal grain size distribution can develop.[12–14] Numerical simulations have been used to verify this idea, which will be referred to as the nucleation-limiting coarsening theory.[14] The purpose of this paper is to test experimentally the predictions of this theory and numerical simulations based on the theory.

The nucleation-limited coarsening theory is based on the idea that a singular crystal surface can only advance or retract by the lateral motion of steps. In the absence of a persistent source of these steps (such as a screw dislocation), a terrace must be nucleated and there will be an energy barrier for this process. The nucleation energy barrier has also been cited as influencing the initial stages of sintering.[15,16] The presence of a barrier during coarsening is consistent with the conventional theory for the growth of crystals from a vapor, a solution, or from a super-cooled melt.[17] The principal difference between the aforementioned growth processes and coarsening is the magnitude of the driving force. The curvature differences that drive coarsening are very small in comparison with the volumetric free energy differences (difference between the material in the precursor phase and the crystal phase) that drive crystal growth processes from a vapor, melt, or solution. In coarsening, the barrier for nucleation depends on the size of the crystal and whether it is growing or dissolving. If the ensemble of coarsening crystals is characterized by the dimension r^*, the size of a crystal that neither shrinks nor grows, one finds that the nucleation energy barrier for adding layers to growing crystals (crystals with sizes greater than r^*) is constant, the barrier for removing layers from shrinking crystals with sizes less than $r^*/2$ is 0, and intermediate barriers for removing layers are found for crystals with sizes between $r^*/2$ and r^*.[14] When estimates of the nucleation energy barrier are compared with the available thermal energy and capillary driving forces, one concludes that micrometer-sized crystals without step-producing defects are unable to grow.[13–16,18–20] This conclusion leads to a situation where two distinct populations of crystals can grow at very different rates: a population containing step sources such as screw dislocations that can grow to large sizes (using the material from the small crystals that dissolve without a barrier), and a population of crystals without step sources that are unable to grow because the nucleation of new layers is kinetically limited. This situation leads to a transient bimodal distribution of grain sizes.

There are four specific predictions from the nucleation-limited coarsening theory that are subject to experimental validation. The first is that the bimodal distribution is transient. In other words, it arises from an initially unimodal distribution that is disrupted when the growth of crystals without step-producing defects is arrested by the nucleation energy barrier. The crystals with step-producing defects continue to grow until all of the smaller and more perfect crystals are dissolved, at which point the distribution becomes unimodal again and consists only of crystals with step-producing defects. The second prediction is that during the period when the distribution is bimodal, there is a constant number density of the larger crystals. In other words, only those crystals with step-producing defects grow and there should be an approximately constant number of these grains. During the same period, the number of the smaller grains should decrease, because they dissolve to feed the growth of the larger crystals. Finally, in the ideal case, the maximum size of the small grains should be constant, as the nucleation energy barrier prevents their growth. However, the constancy of the maximum size assumes that the grains are completely dispersed and that no other growth mechanisms can operate. In practice, crystals will always impinge either because of gravity-driven sedimentation or because their volume fraction exceeds the percolation threshold. It has previously been shown that when faceted crystals contact at their faces, the nucleation barrier is eliminated and they coalesce.[15,16,21] Therefore, the impinging crystals can also grow by the migration of the grain boundaries (to avoid confusion, we will refer to growth by motion of boundaries as grain growth and growth by dissolution and precipitation as coarsening). However, this rate is expected to be slow in comparison with grain growth in a single-phase dense polycrystal with fully

contiguous grains. Therefore, the fourth prediction is more realistically modified to say that the maximum size of the smaller subset of the population should increase slowly at a rate determined by the grain contiguity.

There is already a considerable body of published observations that support the nucleation-limited coarsening theory, and these results have recently been reviewed.[20] What is missing is a comprehensive body of data from a single system that matches the assumptions of the theory as nearly as possible and reduces possible uncertainties. To fulfill these conditions, we have measured the time evolution of the grain size distribution of $SrTiO_3$ in a titania-rich liquid at 1500°C. We have previously reported on the surface energy anisotropy of $SrTiO_3$ in air and found that its (100) surfaces are singular.[22] We have also reported on the evolution of the shapes of $SrTiO_3$ crystals in a titania-rich liquid with the same composition and at the same temperature used in the current experiments and found that the crystals have a large proportion of flat (100) facets.[23] Therefore, this system meets the requirement that bounding surfaces must move by the lateral motion of steps. The coarsening crystals are, however, in contact with one another so, in parallel with the coarsening process, grain growth will also occur. To estimate the rate of this process, we use the grain growth rate in a system with no added second phase as a reference point and assume that in the two-phase system, the grain growth rate will be diminished in proportion to the contiguity.

II. Experimental Procedure

Two-phase $SrTiO_3$–TiO_2 specimens were formulated so that at the annealing temperature of 1500°C, they would consist of a mixture with 85% volume fraction solid $SrTiO_3$ and 15% volume fraction of a titania-rich liquid.[24] In this mixture, the liquid was comprised of 33.3 mol% $SrTiO_3$ and 66.7 mol% TiO_2. To realize this composition, $SrTiO_3$ and TiO_2 powders (99% pure) were mixed and then milled with ethanol and 1 cm glass balls for 5 h. Inspection of the powders at this point by scanning electron microscopy (SEM) showed agglomerates of roughly spherical submicrometer-sized particles with no obvious flat surfaces. After drying, the powder was mixed with a small amount of polyethylene glycol binder and deionized water, and then uniaxially pressed to 11.7 MPa. The consolidated samples were then degassed in vacuum at 800°C for 25 h before annealing in air at 1500°C. The samples were ramped to 1500°C at a rate of 5°C/min and then held at this temperature for times ranging from 0 to 50 h. The samples were then lapped with 3 μm alumina slurry and polished with 0.02 μm colloidal silica slurry. Single-phase $SrTiO_3$ polycrystals were also created to determine grain growth rates in a dense sample. These specimens were prepared by methods identical to those described above, but using only $SrTiO_3$ powder. Before SEM imaging, each sample was lapped, polished, and thermally grooved at 1400°C for 6 min.

To determine the growth rate of crystals known to contain dislocations, plate-shaped single crystals were embedded in powder with the same composition as the two-phase sample. After heating at 1500°C for 5 h, the samples were sectioned perpendicular to the plane of the plate. The original surface of the seed is easily identified by a line of defects, and the amount of growth was determined by measuring the distance that the interface advanced from its original position. The polished surfaces of a plate from the same sample were etched in 50 vol% HNO_3–50 vol% deionized water to form pits at the surface/dislocation intersection. By counting the pits, the dislocation density was determined to be 5×10^5 cm^{-2}.

The grain size distributions in each sample were determined from images obtained using a SEM (XL30 FEG, Phillips, Eindhoven, the Netherlands). To prevent charging, the samples were coated with a thin layer of carbon. All SEM imaging was conducted at a 0° stage tilt and a 20.0 kV accelerating voltage. Various magnifications were used to best image the microstructures. For the 3-, 5-, and 10-h two-phase samples, there was a wide distribution of grain sizes. To make sure the large and small populations were both measured, images of the same areas were recorded at two different magnifications. The linear intercept method was used to calculate the grain size distributions. The liquid-phase lengths along the test lines were subtracted before dividing the number of grains counted along the lines. The mean intercept lengths were stereologically corrected by a factor of 1.5 to yield grain diameters.[25] For specimens where two magnifications were used, all grains below a fixed size (set differently for each distribution) were determined from the high-magnification images. When the grain size data were binned, the bin size was decreased for the data obtained from the higher magnification images. For the two-phase materials, at least 2138 grains were measured in each sample and for the single-phase materials, at least 1353 grains were measured in each sample.

The contiguity of the $SrTiO_3$ crystals in the two-phase samples was determined from crystal orientation maps on planar sections obtained using an electron-backscattered diffraction (EBSD) mapping system (TexSEM Laboratories, Provo, UT) integrated with a SEM (Model XL40 FEG, Phillips). Orientation maps were recorded at a 60° tilt with a 20 kV beam. The step sizes for the orientation mapping were between 0.3 and 1.6 μm, depending on the grain size. The solidified liquid phase did not produce EBSD patterns that could be indexed. In this case, the OIM analysis software (TexSEM Laboratories Inc. version 3.03) assigns low values for the image quality and orientation confidence index parameters. Using these parameters as a guide, the unindexed points were assigned unique Euler angles ($\phi_1 = 0$, $\Phi = 0$, and $\phi_2 = 0$) so that these regions were easy to identify in the later analysis. The orientation data were then processed to remove spurious observations using a "grain dilation clean-up" in the OIM software. A single orientation was then assigned to each $SrTiO_3$ grain by averaging all of the orientations within a single grain that were measured with a confidence index greater than 0.2. The OIM analysis software was then used to extract all boundary line segments. The segments arising from solid–liquid boundaries were easily distinguished from those arising from solid–solid boundaries because of the unique zero Euler angles on one side of the boundary. With the lengths of the solid–solid (L_{s-s}) and solid–liquid (L_{s-l}) interface traces measured in this way, the contiguity can be calculated by the equation[26,27]

$$\text{Contiguity} = \frac{\sum 2L_{s-s}}{\sum [2L_{s-s} + L_{s-l}]} \qquad (1)$$

III. Results

The images in Fig. 1 illustrate the microstructures of the two-phase (Fig. 1(a)) and the single-phase (Fig. 1(b)) samples after 5 h of annealing. The grain size distributions derived from these specimens are shown in Fig. 2. Note that the grain size distribution shown in Fig. 2(a) has two distinct peaks, one at about 9 μm and one at 90 μm, while the one in Fig. 2(b) has a single peak at about 40 μm. These are the characteristic features that we use to determine whether a grain size distribution is bimodal (Fig. 2(a)) or unimodal (Fig. 2(b)). In the single-phase sample, the distribution was unimodal at all times and for the two-phase sample, the distribution was bimodal after 0, 3, 5, and 10 h, but unimodal at longer times. The grain size distributions for two-phase samples heated for 3 and 50 h are compared in Fig. 3 to illustrate the change from bimodal to unimodal. In the analysis of the bimodal distributions that follows, the crystals associated with the first peak will be referred to as the small crystals and those crystals associated with the second peak as the large crystals. Note that although the volume fraction peak associated with the large crystals is always higher than the one associated with the small crystals, the small crystals are far more numerous.

To determine the number of grains per unit volume (N_v), we measured the average number per unit area in a planar section (N_A), and divided by the average diameter (d).[28] The results for the populations of grains associated with each peak in the distribution are shown in Fig. 4. The numbers of the large grains (Fig. 4(a)) and the small grains (Fig. 4(b)) behave very differ-
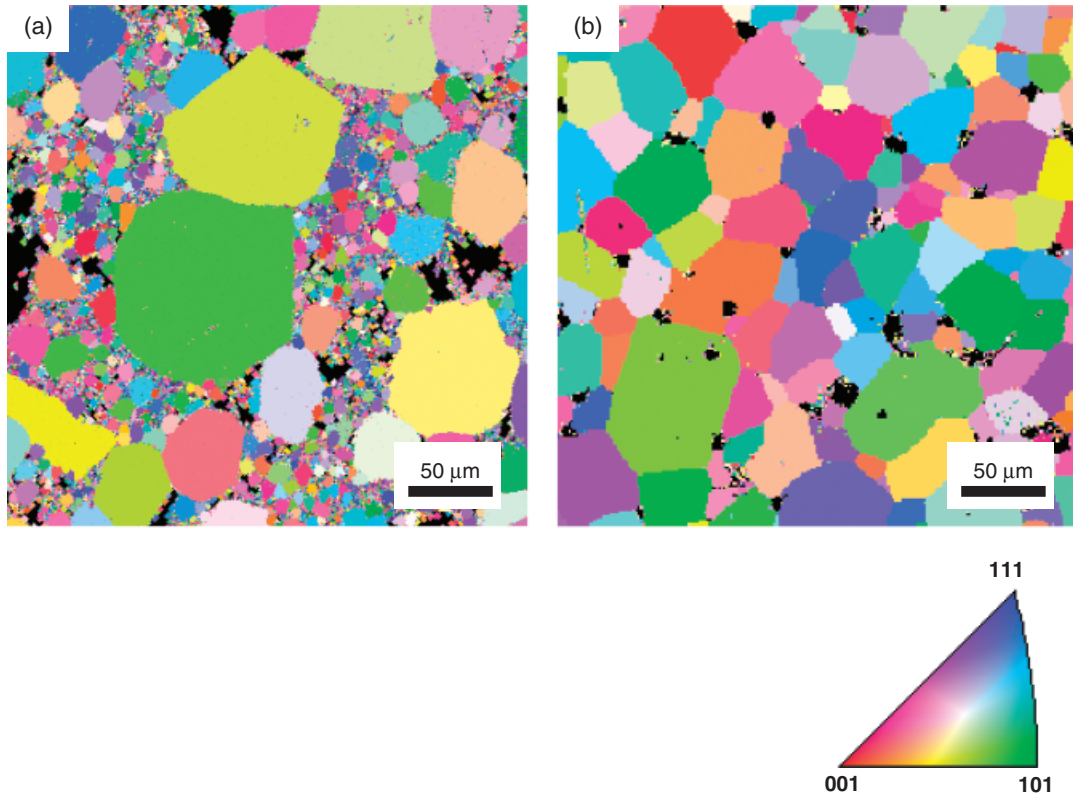
Fig. 1. Inverse pole figure maps show the microstructures of the two-phase (a) and single-phase (b) samples after heating for 5 h at 1500°C. In these maps, the colors indicate the orientation according to the key shown in the unit triangle. The black regions are liquid phase or pores in (a) and pores in (b).

ently as a function of time. In the range of 0–5 h, the number of the large grains is constant within experimental uncertainty. At the same time, the number of small grains decreases rapidly. The density of large grains decreases at 10 h. This is at the point where few small grains remain and the large grains begin to impinge on each other. When this occurs, the large grains also begin to be eliminated. By 15 h, when the distribution is unimodal and no small grains remain, the number of large grains also declines significantly as their average size continues to increase.

The changes in the average sizes of the crystals during the bimodal regime are shown in Fig. 5, which compares the mean sizes of the grains in the single-phase sample with the mean sizes of the large and small grains in the two-phase sample. The large grains in the two-phase sample grow the fastest, the small grains in the two-phase sample grow the slowest, and the grains in the single-phase sample have an intermediate growth rate. As mentioned previously, the distributions in the single-phase and two-phase sample are unimodal after 10 h. The average grain sizes continue to increase, but a distinct population of small crystals can no longer be distinguished in the two-phase sample. The unimodal condition remained even at the longest time examined (50 h).

An EBSD map of a section perpendicular to the plate of a seeded sample with the (100) orientation is shown in Fig. 6. This experiment was also carried out on samples with (111) orientations. However, because the (100)-oriented crystals grew the least, the (100) sample was selected as representative of the process that would limit the growth of an equiaxed, three-dimensional (3D) crystal. The newly grown crystal has a columnar structure with low-angle grain boundaries (less than 1° of misorientation) between the columns. By averaging the amount
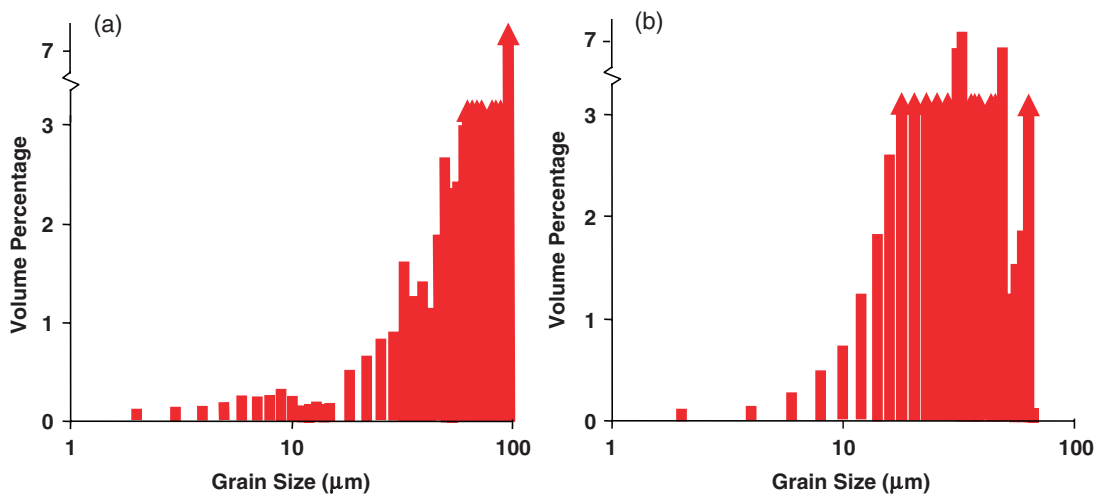
Fig. 2. Grain size distributions from the two-phase (a) and the single-phase (b) sample after heating for 5 h at 1500°C. Bars ending with arrows are grain sizes that have volume percentages between 3 and 7, or above 7.
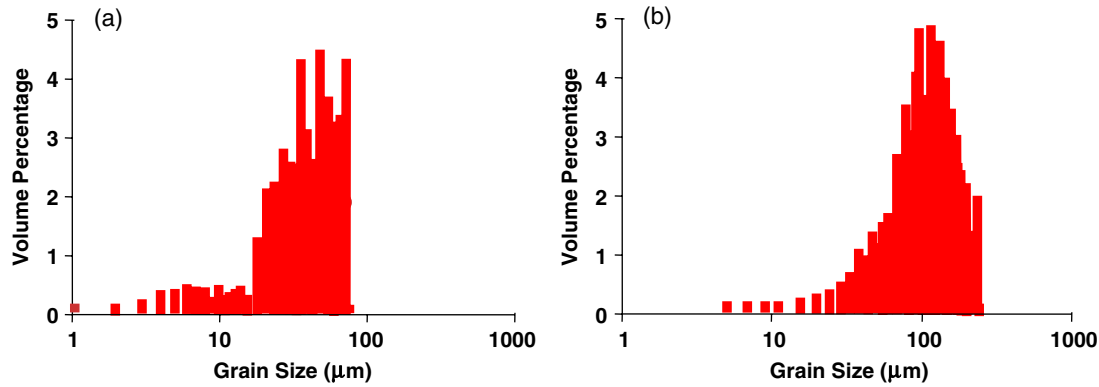
Fig. 3. Comparison of the grain size distributions from the two-phase sample after 3 h (a) and after 50 h (b) to illustrate the transient character of the bimodal distribution.

of growth at several places along the interface on two samples, the growth during a 5-h period was determined to be 170 μm. The (111)-oriented sample grew almost 300 μm under the same conditions.

IV. Discussion

The observations of SrTiO$_3$ coarsening in a titania-rich liquid are consistent with the predictions of the nucleation-limited coarsening theory. The first prediction is that during isothermal heating, a bimodal distribution arises out of an initially uni-modal distribution and, when the small crystals in the distribution are exhausted, the distribution becomes unimodal again. The starting powders were thoroughly milled and microscopic inspection indicated that the distribution of grain sizes was uniform. After heating the sample to 1500°C and back to room temperature, 10 μm grains could be found among grains whose average size was less than 2 μm. In other words, the bimodal distribution appeared in the very initial stages of growth. After 10 h, the distribution again becomes unimodal; the two types of distributions are illustrated in Fig. 3. Thus, a transient bimodal distribution is observed in this system.

The second prediction is that during the period where the bimodal distribution is present, there is a constant number of the larger crystals. The observations in Fig. 4(a) are consistent with this prediction. Note that in the first 5 h of annealing, the average sizes of the large grains increase from about 5 μm to about 20 μm. Because the number of these crystals remains constant, the mass conservation requirement allows us to conclude that the material for this growth arises entirely from the population of smaller crystals. The decrease in the number of the large crystals that is observed at 10 and 15 h indicates that at this point, the material needed for continued growth must be derived from the smallest of the large crystals. Because the large grains impinge at this point, some of this growth will also occur by the motion of grain boundaries. The third prediction is that the number density of the smaller grains should decrease, because they dissolve to feed the growth of the larger population. The data in Fig. 4(b) are consistent with this prediction.

The fourth and final prediction is that the maximum size of the small grains should be constant, as the nucleation energy
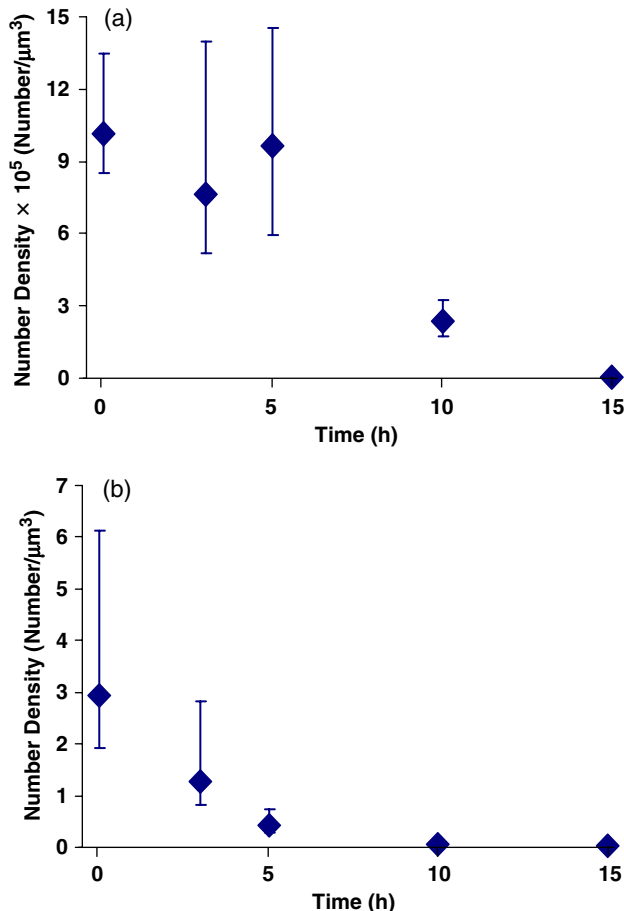
Fig. 4. Number of large (a) and small (b) grains per unit volume in the two-phase sample as a function of time after heating at 1500°C. The points represent the mean values of N_v, while the bars represent one standard deviation above and below the mean, derived from the measurements of the diameter.
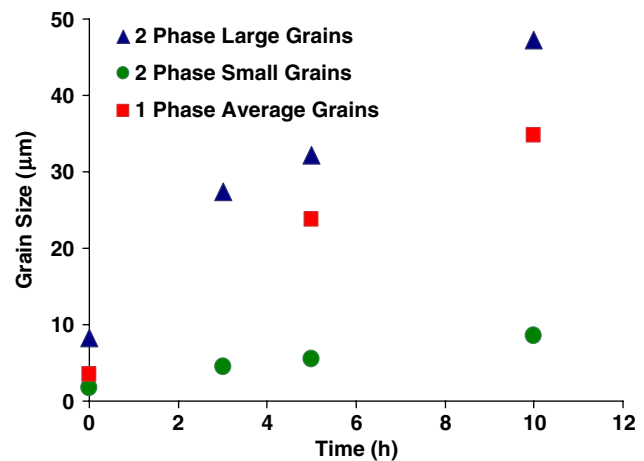
Fig. 5. Average sizes of the large grains in the two-phase sample (blue triangles), the small grains in the two-phase sample (green circles), the grains in the single-phase sample (red squares), as a function of time at 1500°C.
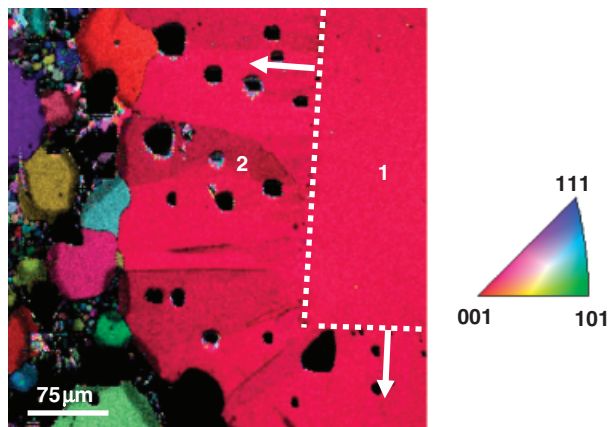
Fig. 6. Electron-backscattered diffraction inverse pole figure map showing a transverse section through the deliberately seeded sample, heated for 5 h at 1500°C. The seed crystal is labeled 1 and the grown area is labeled 2, with arrows indicating the direction of growth. The contrast in the micrograph combines both orientation (color) and the quality of the backscattered pattern used to measure the orientation (brightness). Differences in the pattern quality allow small misorientations to be visualized.

barrier prevents their growth by coarsening. However, as noted in Section I, this can only be true in the case where the crystals are not in contact with each other. Because it is impossible to obtain this condition in the experiment, we expect some growth by grain boundary migration.[15,16,21] Further, because of the reduced contiguity, this rate is expected to be less than what would occur in a fully contiguous sample at the same temperature. The grain growth expectation is verified by the data in Fig. 5, which show that the small grains grow much more slowly than the grains in a dense polycrystal.

It is possible to make an estimate of how fast the average grain size of the small grains should increase if they grow only by grain boundary migration. The growth law for the single-phase system, determined by fitting to the measured mean grain size, $\langle r \rangle$, is:

$$\langle r \rangle = 15.7 t^{0.33} \qquad (2)$$

where t is the time in hours and $\langle r \rangle$ is measured in micrometers. The contiguity of the $SrTiO_3$ crystals was determined to be 0.4. Hence, grain boundaries comprise 40% of the total bounding interface area. Assuming that 40% of a crystal's bounding surface area advances as a rate given by Eq. (2) and that this added volume is then distributed uniformly over the entire crystal, new
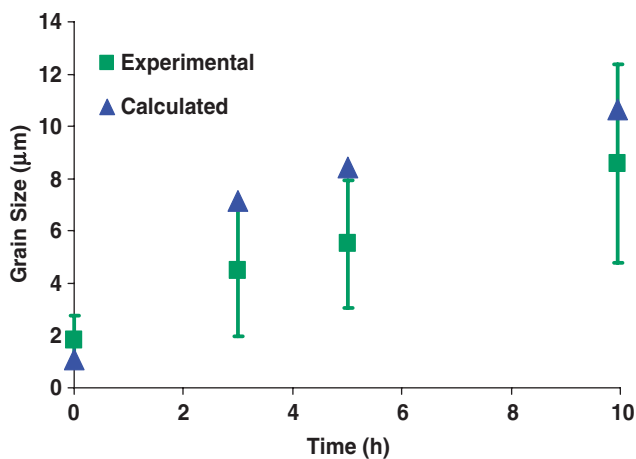
Fig. 7. Average sizes of the small grains in the two-phase sample (green squares) as a function of time compared with the grains sizes calculated from the growth rate of grains in the single-phase sample (blue triangles), modified for the effect of reduced contiguity.

radii can be calculated for each annealing time. This method of estimating the rate of grain growth in a polycrystal with low contiguity is admittedly approximate, but should provide an upper limit for the rate at which grain boundary motion could lead to an increase in the grain size. When the predicted growth (blue triangles) and the observed growth (green squares) are compared (see Fig. 7), we see that they are consistent. In other words, the small amount of growth of the smaller crystals could be explained by grain boundary motion in the absence of coarsening that is blocked by the nucleation energy barrier.

It is assumed that the grains that grow rapidly have screw dislocations emerging on their surfaces so that the nucleation energy barrier does not affect their growth. In the initially milled powder, it is safe to assume that there is considerable disorder. In the initial stages of heating, however, dislocations in these submicrometer crystals are also likely to be driven to interfaces by image forces and annihilated. If some grains retain dislocations, then these can act as seeds for the growth of the large grains in the population. This allows us to pose the question: what is the minimum density of dislocations that would be required in the initial state to create the observed microstructure? If we compare the relative number densities of the small and large grains in the 0-h sample, we find that there are 30 000 times more small grains than large grains. So, assuming that at least one cube-shaped grain with an edge length of about 1 μm has three threading dislocations, and that the other similarly shaped 30 000 grains are perfect, the necessary dislocation density is 3 μm per 30 000 cubic micrometers or 10^4 cm^{-2}. Note that this estimate is a lower bound, not including the dislocations that do not create effective step sources (for example, edge dislocations with line directions perpendicular to the surface). By counting etch pits, we have measured dislocation densities in $SrTiO_3$ single crystals to be as high as 5×10^5 cm^{-2} and this is consistent with our analysis of etch pit distributions in other work.[29] Therefore, the minimum density of dislocations required to produce the observed microstructure by nucleation-limited coarsening is plausible. It is also worth pointing out that if crystals containing the appropriate defects are too numerous, the bimodal transient will occur very quickly and is not likely to be observed. Only when the defects are relatively rare will the bimodal distribution be sustained long enough to be observed.

The nucleation energy barrier will arrest the growth of the defect-free crystals only if it is sufficiently larger than the available thermal energy and the capillary driving force. Assuming a temperature of 1500°C, a step height of 2 Å, and that the energy of the step scales directly with the surface energy (assumed to be 0.1 J/m^2), then the nucleation energy barrier is in the range of 10^3 kT.[14] Assuming an average grain size of 0.5 μm, the energy barrier is 10^5 times the mean field capillary driving force. Under these conditions, nucleation is clearly not feasible.[18,20] The only parameter in doubt in this estimate is the energy of the step. However, the step energy would have to be more than 20 times lower than the assumed value (0.1 J/m^2) for nucleation to occur at a reasonable rate and this does not seem plausible. Impurities are known to affect step energies strongly and it is possible that they may reduce the step energy enough to allow nucleation. However, if this was the case, then 2D growth should occur on all grains rather than a small minority and it is therefore not possible to explain the bimodal distribution. Similarly, if the roughening temperature was exceeded and the barrier disappeared, growth would occur uniformly and the distribution would be unimodal.

To test whether or not crystals known to have dislocations grow at a rate similar to the large grains in these samples that are assumed to contain dislocations, a macroscopic single-crystal seed was embedded in a matrix of the same composition as the rest of the two-phase samples and heated for 5 h. The interface of this crystal advanced 170 μm. Etch pit studies confirmed that the macroscopic seed contained dislocations. If a much smaller grain also possessed the requisite dislocations, its bounding surfaces should advance by a similar distance. A sample that was treated in exactly the same way, but with no added seed,

was also examined. On a single section plane through this sample, a grain with an apparent diameter of 140 µm was observed. Because the 3D shape of this crystal was not known, it is impossible to know the true diameter. However, the amount that this crystal grew is comparable with the amount that the macroscopic seed grew, confirming the idea that a relatively small crystal that is assumed to contain dislocations can grow just as much as a much larger crystal known to have dislocations.

The observations compiled here are consistent with previous reports in the literature. For example, Rehrig *et al.*[30] have reported a transient bimodal grain size distribution in $BaTiO_3$ coarsening under conditions where an intergranular liquid is expected. In this experiment, the largest $BaTiO_3$ crystals grow while those in the small population are practically stagnant before they disappear. In the present case, we have based our analysis on complete grain size distribution data and added measurements of the number density of the fastest-growing grains. The nucleation-limited coarsening theory can also provide an explanation for the fact that 65 mol% $Pb(Mg_{1/3}Nb_{2/3})O_3$–35 mol% $PbTiO_3$ seeds added to a fine-grained matrix containing a liquid phase grow many times faster than the matrix[31]: the seeds, by virtue of their size, are guaranteed to have the step-producing defects needed to eliminate the nucleation energy barrier. The finer grains, on the other hand, are less likely to have these defects and this may explain why the growth of these grains stagnates at relatively small sizes.[32,33]

V.   Conclusions

As a test of the nucleation-limited coarsening theory, the time evolution of the grain size distribution has been measured for $SrTiO_3$ crystals coarsening in a titania-rich liquid. Initially, a bimodal grain size distribution develops. During this period, a constant number of large crystals grow at the expense of a diminishing population of small crystals. After the small crystals are exhausted, the large crystals continue to coarsen and exhibit a unimodal grain size distribution. The slow increase in the average size of the small crystals that occurs before they are exhausted can be explained by grain boundary migration. These observations are consistent with the nucleation-limited coarsening theory, which provides a plausible explanation for the development of transient bimodal grain size distributions in systems of crystals bounded by singular surfaces.

References

[1] I. M. Lifshitz and V. V. Slyozov, "The Kinetics of Precipitation from Supersaturated Solid Solutions," *J. Phys. Chem. Solids*, **19** [1/2] 33–40 (1961).

[2] C. Wagner, "Theorie der Alterung von Niederschlägen durch Umlösen (Ostwald-Reifung)," *Z. Elektrochemie*, **65** [7/8] 581–91 (1961).

[3] G. J. Shiflet, H. I. Aaronson, and T. H. Courtney, "Kinetics of Coarsening by the Ledge Mechanism," *Acta Metall.*, **27** [3] 377–85 (1979).

[4] A. J. Ardell, "The Effect of Volume Fraction on Particle Coarsening: Theoretical Considerations," *Acta Metall.*, **20** [1] 61–71 (1972).

[5] A. D. Brailsford and P. Wynblatt, "The Dependence of Ostwald Ripening Kinetics on Particle Volume Fraction," *Acta Metall.*, **27** [3] 489–97 (1979).

[6] C. K. L. Davies, P. Nash, and R. N. Stevens, "The Effect of Volume Fraction of Precipitate on Ostwald Ripening," *Acta Metall.*, **28** [2] 179–89 (1980).

[7] K. Tsumuraya and Y. Miyata, "Coarsening Models Incorporating Both Diffusion Geometry and Volume Fraction of Particles," *Acta Metall.*, **31** [3] 437–52 (1983).

[8] P. W. Voorhees and M. E. Glicksman, "Solution to the Multi-Particle Diffusion Problem With Applications to Ostwald Ripening. I. Theory," *Acta Metall.*, **32** [11] 2001–11 (1984).

[9] W. W. Mullins, "The Statistical Self Similarity Hypothesis in Grain Growth and Particle Coarsening," *J. Appl. Phys.*, **59** [4] 1341–9 (1986).

[10] A. D. Rutenberg and B. P. Vollmayr-Lee, "Anisotropic Coarsening: Grain Shapes and Nonuniversal Persistence," *Phys. Rev. Lett.*, **83** [19] 3772–5 (1999).

[11] E. Brosh and R. Z. Shneck, "Anisotropic Coarsening: The Effect of Interfacial Properties on the Shape of Grains," *Model. Simul. Mater. Sci. Eng.*, **8** [6] 815–23 (2000).

[12] G. S. Rohrer and W. W. Mullins, "Recrystallization and Grain Growth"; pp. 321–6 in *Proceedings of the First Joint International Conference*, Edited by G. Gottstein and D. A. Molodov. Springer Verlag, Berlin, 2001.

[13] B. W. Sheldon and J. Rankin, "Step-Energy Barriers and Particle Shape Changes during Coarsening," *J. Am. Ceram. Soc.*, **85** [3] 683–90 (2002).

[14] G. S. Rohrer, C. L. Rohrer, and W. W. Mullins, "Coarsening of Faceted Crystals," *J. Am. Ceram. Soc.*, **85** [3] 675–82 (2002).

[15] J. Rankin and B. W. Sheldon, "Surface Roughening and Unstable Neck Formation in Faceted Particles: I, Experimental Results and Mechanism," *J. Am. Ceram. Soc.*, **82** [7] 1868–72 (1999).

[16] B. W. Sheldon and J. Rankin, "Surface Roughening and Unstable Neck Formation in Faceted Particles: II, Mathematical Modeling," *J. Am. Ceram. Soc.*, **82** [7] 1873–8 (1999).

[17] W. K. Burton, N. Cabrera, and F. C. Frank, "The Growth of Crystals and the Equilibrium Structure of Their Surfaces," *Philos. Trans. R. Soc. London, Ser. A*, **243**, 300–58 (1951).

[18] W. W. Mullins and G. S. Rohrer, "Nucleation Barrier for Volume Conserving Shape Changes of Faceted Crystals," *J. Am. Ceram. Soc.*, **83** [1] 214–6 (2000).

[19] G. S. Rohrer, C. L. Rohrer, and W. W. Mullins, "Nucleation Energy Barriers for Volume Conserving Shape Changes of Crystals with Nonequilibrium Morphologies," *J. Am. Ceram. Soc.*, **84** [9] 2099–104 (2001).

[20] G. S. Rohrer, "Influence of Interface Anisotropy on Grain Growth and Coarsening," *Annu. Rev. Mater. Res.*, **35**, 99–126 (2005).

[21] J. Rankin and L. A. Boatner, "Unstable Neck Formation During Initial-Stage Sintering," *J. Am. Ceram. Soc.*, **77** [8] 1987–90 (1994).

[22] T. Sano, D. M. Saylor, and G. S. Rohrer, "Surface Energy Anisotropy of $SrTiO_3$ at 1400°C in Air," *J. Am. Ceram. Soc.*, **86** [11] 1933–9 (2003).

[23] T. Sano, C.-S. Kim, and G. S. Rohrer, "Shape Evolution of $SrTiO_3$ Crystals During Coarsening in a Titania-Rich Liquid," *J. Am. Ceram. Soc.*, **88** [4] 993–6 (2005).

[24] *Phase Diagrams for Ceramists 1969 Supplement*, Edited by M. K. Reser. American Ceramic Society, Columbus, OH, 1969 (Figure 2334).

[25] E. E. Underwood, *Quantitative Stereology*, pp. 90–91. Addison-Wesley Publishing Co., Reading, MA, 1970.

[26] J. Gurland, "An Estimate of Contact and Contiguity of Dispersions in Opaque Samples," *Trans. Metall. Soc. AIME*, **236** [5] 642–6 (1966).

[27] R. M. German, "The Contiguity of Liquid Phase Sintered Microstructures," *Metall. Trans. A*, **16A** [7] 1247–52 (1985).

[28] J. C. Russ, *Practical Stereology*, p. 54. Plenum Press, New York, NY, 1986.

[29] S.-Y. Chung and S–J. L. Kang, "Effect of Dislocations on Grain Growth in $SrTiO_3$," *J. Am. Ceram. Soc.*, **83** [11] 2828–32 (2000).

[30] P. W. Rehrig, G. L. Messing, and S. Trolier-McKinstry, "Templated Grain Growth of Barium Titanate Single Crystals," *J. Am. Ceram. Soc.*, **83** [11] 2654–60 (2000).

[31] P. T. King, E. P. Gorzkowski, A. M. Scotch, D. J. Rockosi, H. M. Chan, and M. P. Harmer, "Kinetics of {001} $Pb(Mg_{1/3}Nb_{2/3})O_3$–35 mol% $PbTiO_3$ Single Crystals Grown by Seeded Polycrystal Conversion," *J. Am. Ceram. Soc.*, **86** [12] 2182–7 (2003).

[32] E. M. Sabolsky, G. L. Messing, and S. Trolier-McKinstry, "Kinetics of Templated Grain Growth of 0.65 $Pb(Mg_{1/3}Nb_{2/3})O_3$–0.35$PbTiO_3$," *J. Am. Ceram. Soc.*, **84** [11] 2507–13 (2001).

[33] J. S. Wallace, J.-M. Huh, J. E. Blendell, and C. A. Handwerker, "Grain Growth and Twin Formation in 0.74PMN·0.26PT," *J. Am. Ceram. Soc.*, **85** [6] 1581–4 (2002).   ☐